Office de la Propriété Intellectuelle du Canada
Un organisme d'Industrie Canada

Canadian Intellectual Property Office
An agency of Industry Canada

CA 2881807 C 2017/10/17

(11)(21) 2 881 807

(12) BREVET CANADIEN
CANADIAN PATENT

(13) C

(86) Date de dépôt PCT/PCT Filing Date: 2012/08/17
(87) Date publication PCT/PCT Publication Date: 2014/02/20
(45) Date de délivrance/Issue Date: 2017/10/17
(85) Entrée phase nationale/National Entry: 2015/02/11
(86) N° demande PCT/PCT Application No.: US 2012/051387
(87) N° publication PCT/PCT Publication No.: 2014/028030

(51) Cl.Int./Int.Cl. *G01V 1/34* (2006.01)

(72) Inventeurs/Inventors:
JIANG, FAN, US;
JIN, SHENGWEN, US

(73) Propriétaire/Owner:
LANDMARK GRAPHICS CORPORATION, US

(74) Agent: NORTON ROSE FULBRIGHT CANADA LLP/S.E.N.C.R.L., S.R.L.

(54) Titre : SYSTEMES ET PROCEDES PERMETTANT D'IMAGER DES DONNEES SISMIQUES
(54) Title: SYSTEMS AND METHODS FOR IMAGING SEISMIC DATA

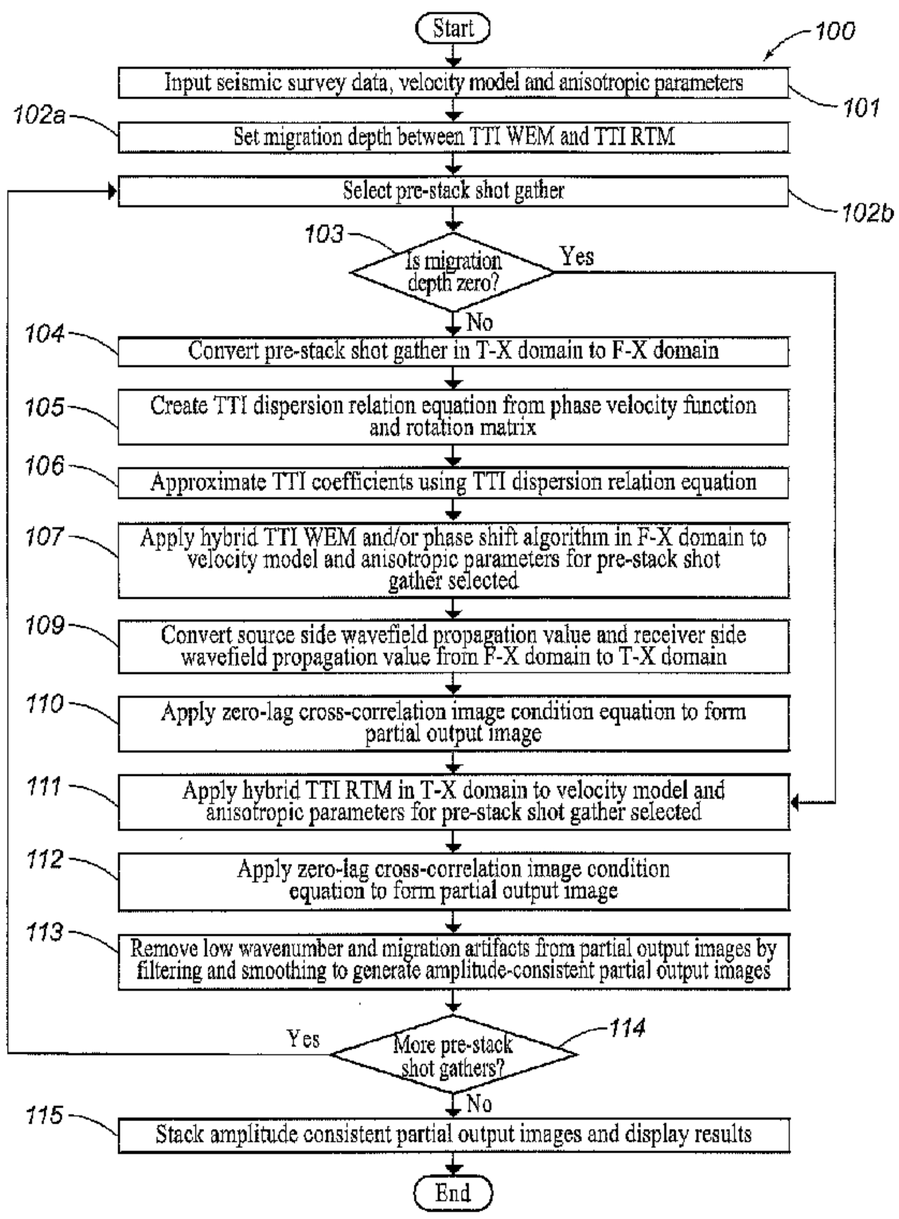


(57) Abrégé/Abstract:
Systems and methods for imaging seismic data using hybrid one-way wave-equation-migration in tilted transverse isotropic media and/or hybrid two-way reverse-time-migration in tilted transverse isotropic media.

(12) INTERNATIONAL APPLICATION PUBLISHED UNDER THE PATENT COOPERATION TREATY (PCT)

(19) World Intellectual Property Organization
International Bureau

(43) International Publication Date
20 February 2014 (20.02.2014)

WIPO | PCT

(10) International Publication Number
WO 2014/028030 A1

(51) **International Patent Classification**:
*G01V 1/00* (2006.01)

(21) **International Application Number**:
PCT/US2012/051387

(22) **International Filing Date**:
17 August 2012 (17.08.2012)

(25) **Filing Language**: English

(26) **Publication Language**: English

(71) **Applicant** *(for all designated States except US)*: **LANDMARK GRAPHICS CORPORATION** [US/US]; 2107 CityWest Blvd. Bldg. 2, Houston, TX 77042 (US).

(72) **Inventors; and**
(75) **Inventors/Applicants** *(for US only)*: **JIANG, Fan** [CN/US]; 6830 Delander Way, Sugar Land, TX 77479 (US). **JIN, Shengwen** [CN/US]; 5226 Harvest Bend Ct., Sugar Land, TX 77479 (US).

(74) **Agent**: **JENSEN, William, P.**; Crain, Caton & James, 1401 McKinney Street, Suite 1700, Houston, TX 77010 (US).

(81) **Designated States** *(unless otherwise indicated, for every kind of national protection available)*: AE, AG, AL, AM, AO, AT, AU, AZ, BA, BB, BG, BH, BN, BR, BW, BY, BZ, CA, CH, CL, CN, CO, CR, CU, CZ, DE, DK, DM, DO, DZ, EC, EE, EG, ES, FI, GB, GD, GE, GH, GM, GT, HN, HR, HU, ID, IL, IN, IS, JP, KE, KG, KM, KN, KP, KR, KZ, LA, LC, LK, LR, LS, LT, LU, LY, MA, MD, ME, MG, MK, MN, MW, MX, MY, MZ, NA, NG, NI, NO, NZ, OM, PE, PG, PH, PL, PT, QA, RO, RS, RU, RW, SC, SD, SE, SG, SK, SL, SM, ST, SV, SY, TH, TJ, TM, TN, TR, TT, TZ, UA, UG, US, UZ, VC, VN, ZA, ZM, ZW.

(84) **Designated States** *(unless otherwise indicated, for every kind of regional protection available)*: ARIPO (BW, GH, GM, KE, LR, LS, MW, MZ, NA, RW, SD, SL, SZ, TZ,

*[Continued on next page]*

(54) **Title**: SYSTEMS AND METHODS FOR IMAGING SEISMIC DATA

(57) **Abstract**: Systems and methods for imaging seismic data using hybrid one-way wave-equation-migration in tilted transverse isotropic media and/or hybrid two-way reverse-time-migration in tilted transverse isotropic media.

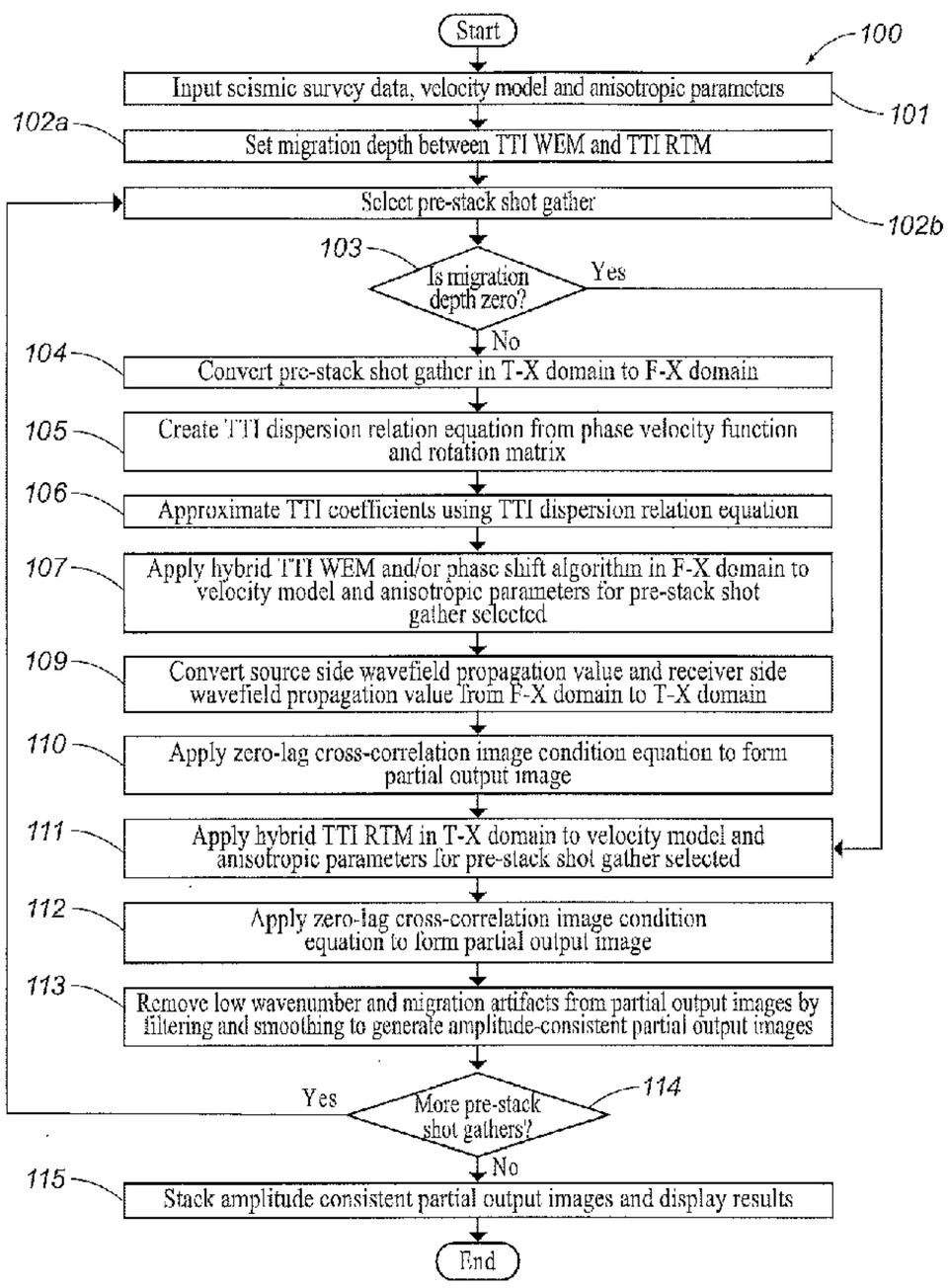


*FIG. 1*

WO 2014/028030 A1

WO 2014/028030 A1

UG, ZM, ZW), Eurasian (AM, AZ, BY, KG, KZ, RU, TJ, TM), European (AL, AT, BE, BG, CH, CY, CZ, DE, DK, EE, ES, FI, FR, GB, GR, HR, HU, IE, IS, IT, LT, LU, LV, MC, MK, MT, NL, NO, PL, PT, RO, RS, SE, SI, SK, SM, TR), OAPI (BF, BJ, CF, CG, CI, CM, GA, GN, GQ, GW, ML, MR, NE, SN, TD, TG).

**Published**:

— *with international search report (Art. 21(3))*

# SYSTEMS AND METHODS FOR IMAGING SEISMIC DATA

## CROSS-REFERENCE TO RELATED APPLICATIONS

[0001] Not applicable.

## STATEMENT REGARDING FEDERALLY SPONSORED RESEARCH

[0002] Not applicable.

## FIELD OF THE INVENTION

[0003] The present invention generally relates to systems and methods for imaging seismic data. More particularly, the present invention relates to imaging seismic data using hybrid one-way wave equation migration in tilted transverse isotropic media ("hybrid TTI-WEM") and/or hybrid two-way reverse time migration in tilted transverse isotropic media ("hybrid TTI-RTM").

## BACKGROUND OF THE INVENTION

[0004] As a commonly applied technique for imaging seismic data, conventional tilted transverse isotropic ("TTI") reverse time migration ("RTM") (collectively "TTI-RTM") propagates a source wave field forward in time and a receiver wave field backward in time to image the subsurface reflector by any well-known two-way wave equation such as the two-way wave equation described in the paper "*Reverse Time Migration: Geophysics*" by Baysal, et al. and in the paper "*Migration by Extrapolation of Time-Dependent Boundary Values: Geophysical Prospecting*" by G. A. McMechan. Although wave equation migration and/or reverse time migration are referred to herein as two-way, they may also be referred to as full-way. In the paper "*Acoustic Approximations for Processing in Transversely Isotropic Media*" by T. Aikhalifah, for example, conventional TTI-RTM is referenced to propose a pseudo-acoustic

approximation in transversely isotropic media with a vertical axis ("VTI"). Based on the pseudo-acoustic approximation in VTI media, research such as, for example, that described in the papers "*An Anisotropic Acoustic Wave Equation for Modeling and Migration in 2D TTI Media*" by Zhou, et al. and "*Reverse Time Migration in Tilted Transversely Isotropic (TTI) Media*" by Fletcher, et al. extended this approximation from VTI to TTI media. These techniques enable structures with strong anisotropy to be imaged. Although conventional TTI-RTM has been applied widely, the computation cost and storage for wavefields are still disadvantages for current computer systems. In other words, the computation cost and memory requirement are still problems for large dataset migration, especially for three-dimensional ("3D") conventional TTI-RTM.

[0005] Instead of a two-way wave equation associated with conventional TTI-RTM, a one-way wave equation can provide faster processing and handle strong lateral velocity variation. One-way wave equations, such as a Finite Difference propagator, a Phase-Shift-Plus-Interpolation propagator, and/or a Generalized Screen propagator, demonstrate good accuracy in general. By extending the one-way isotropic wave equation migration ("WEM") to TTI-WEM as described in the papers "*3D Wavefield Extrapolation in Laterally Varying Tilted TI Media*" by San, et al., "*Implicit Wave Equation Migration in TTI Media Using High Order Operators*" by A. A. Valenciano, and "*3D TTI Implicit Finite Difference Migration With Nonlinear Optimized Four-Direction Splitting Expansion*" by Hua, et al., one-way WEM is able to produce an anisotropic image with high efficiency. Nevertheless, because the one-way WEM ignores up-going waves, one-way WEM fails to handle extremely complex structures, such as steeply dip events and overturned reflectors.

[0006] To combine the advantages of one-way WEM and two-way WEM, a hybrid propagator for prestack migration in isotropic media was developed and is described in the paper "*Hybrid One-Way and Full-Way Wave Equation Propagator and Prestack Migration*" by Luo and Jin ("*Luo and Jin*"). The hybrid propagator combines one-way and two-way WEM to extrapolate a wavefield progressively. In this manner, a one-way propagator may be applied to less complex media while the two-way propagator may be applied to extremely complicated media. Although the use of the *Luo and Jin* hybrid propagator in isotropic media generates comparable image results with two-way WEM for RTM with less noise and computational costs, it has not been applied to TTI media. Moreover, the *Luo and Jin* hybrid propagator does not contemplate the use of Pade approximation, which could provide maximum accuracy for wave propagation.

## SUMMARY OF THE INVENTION

[0007] The present invention therefore, meets the above needs and overcomes one or more deficiencies in the prior art by providing systems and methods for imaging seismic data using hybrid TTI-WEM and/or hybrid TTI-RTM.

[0008] In one embodiment, the present invention includes a method for imaging seismic data, which comprises: i) approximating TTI coefficients using a Pade approximation and a dispersion relation equation; ii) applying hybrid TTI-WEM to a velocity model and anisotropic parameters for a pre-stack shot gather using the approximated TTI coefficients and a computer system to determine a source side wavefield propagation value and a receiver side wavefield propagation value in a frequency-space domain; iii) converting the source side wavefield propagation value and the receiver side wavefield propagation value from the frequency-space domain to a time-space domain; and iv) applying a zero-lag cross-correlation image condition

equation to form a partial output image using the converted source side wavefield propagation value and the converted receiver side wavefield propagation value.

[0009] In another embodiment, the present invention includes a non-transitory program carrier device tangibly carrying computer executable instructions for imaging seismic data, the instructions being executable to implement: i) approximating TTI coefficients using a Pade approximation and a dispersion relation equation; ii) applying hybrid TTI-WEM to a velocity model and anisotropic parameters for a pre-stack shot gather using the approximated TTI coefficients and a computer system to determine a source side wavefield propagation value and a receiver side wavefield propagation value in a frequency-space domain; iii) converting the source side wavefield propagation value and the receiver side wavefield propagation value from the frequency-space domain to a time-space domain; and iv) applying a zero-lag cross-correlation image condition equation to form a partial output image using the converted source side wavefield propagation value and the converted receiver side wavefield propagation value.

[0010] Additional aspects, advantages and embodiments of the invention will become apparent to those skilled in the art from the following description of the various embodiments and related drawings.

## BRIEF DESCRIPTION OF THE DRAWINGS

[0011] The present invention is described below with references to the accompanying drawings in which like elements are referenced with like reference numerals, and in which:

[0012] **FIG. 1** is a flow diagram illustrating one embodiment of a method for implementing the present invention.

[0013] **FIG. 2A** is an image illustrating an exemplary velocity model.

[0014] **FIG. 2B** is an image illustrating an anisotropic parameter epsilon (ε) for the velocity model in **FIG. 2A**.

[0015] **FIG. 2C** is an image illustrating an anisotropic parameter delta (δ) for the velocity model in **FIG. 2A**.

[0016] **FIG. 2D** is an image illustrating an anisotropic parameter theta (θ) for the velocity model in **FIG. 2A**.

[0017] **FIG. 3A** is an image illustrating the results of conventional hybrid one-way WEM and conventional two-way RTM in isotropic media.

[0018] **FIG. 3B** is an image illustrating the results of conventional hybrid one-way WEM and conventional two-way RTM in VTI media.

[0019] **FIG. 3C** is an image illustrating the results of the method in **FIG. 1**.

[0020] **FIG. 3D** is an image illustrating the results of conventional two-way RTM in TTI media.

[0021] **FIG. 4A** is an image illustrating the results of conventional two-way TTI-RTM.

[0022] **FIG. 4B** is an image illustrating the results of the method in **FIG. 1**.

[0023] **FIG. 5** is a flow diagram illustrating one embodiment of a method for implementing step **106** in **FIG. 1**.

[0024] **FIG. 6** is a block diagram illustrating one embodiment of a system for implementing the present invention.

## DETAILED DESCRIPTION OF THE PREFERRED EMBODIMENTS

[0025] The subject matter of the present invention is described with specificity, however, the description itself is not intended to limit the scope of the invention. The subject matter thus, might also be embodied in other ways, to include different steps or combinations of steps similar

to the ones described herein, in conjunction with other technologies. Moreover, although the term "step" may be used herein to describe different elements of methods employed, the term should not be interpreted as implying any particular order among or between various steps herein disclosed unless otherwise expressly limited by the description to a particular order. While the following description refers to the oil and gas industry, the systems and methods of the present invention are not limited thereto and may also be applied to other industries to achieve similar results.

[0026] The present invention significantly reduces the computational time associated with conventional two-way TTI-RTM by applying a hybrid TTI-WEM with an implicit finite difference algorithm and by applying a hybrid TTI-RTM with an explicit finite difference algorithm. The present invention also provides better image quality with less artifacts and can also handle geological topography naturally.

## Method Description

[0027] Referring now to **FIG. 1**, a flow diagram of one embodiment of a method **100** for implementing the present invention is illustrated.

[0028] In step **101**, seismic survey data such as, for example, prestack shot gathers in time-space ("T-X") domain, a velocity model and anisotropic parameters such as, for example, epsilon (ε), delta (δ), tilted dip angle (θ) and azimuth angle (φ) are input using the client interface and/or the video interface described further in reference to **FIG. 6**.

[0029] In step **102a,** a migration depth is set between the hybrid TTI-WEM and the hybrid TTI-RTM using the client interface and/or the video interface described further in reference to **FIG. 6**. The migration depth may be used to separate the velocity model and anisotropic parameters into an area where the hybrid TTI-WEM will be applied from a surface of

the earth to the migration depth below the surface and an area where the hybrid TTI-RTM will be applied below the migration depth to an extent of the velocity model.

[0030] In step **102b**, a prestack shot gather is selected from the prestack shot gathers in step **101** using the client interface and/or video interface described further in reference to **FIG. 6**. Alternatively, the prestack shot gather may be selected automatically. In either event, it may be selected at random or in any other predetermined manner.

[0031] In step **103**, the method **100** determines if the migration depth is zero. If the migration depth is zero, then the method **100** proceeds to step **111** where only the hybrid TTI-RTM will be applied in the T-X domain to the prestack shot gather selected in step **102b** using the velocity model and anisotropic parameters from a surface of the earth to the extent of the velocity model. If the migration depth is not zero, then the method **100** proceeds to step **104** where the hybrid TTI-WEM will be applied in the frequency-space ("F-X") domain to the prestack shot gather selected in step **102b** using the velocity model and anisotropic parameters from a surface of the earth to the migration depth and the hybrid TTI-RTM will be applied in the T-X domain to the prestack shot gather selected in step **102b** using the velocity model and anisotropic parameters from the migration depth to the extent of the velocity model.

[0032] In step **104**, the prestack shot gather selected in step **102b** is converted from its native T-X domain to the F-X domain using techniques well-known in the art such as, for example, a fast fourier transform ("FFT") algorithm.

[0033] In step **105**, a TTI dispersion relation equation, which is also be referred to as a quartic equation, is created from the well-known phase velocity function and rotation matrix. By extending dispersion relation in laterally varying TTI media to 3D TTI media, including varying

dip angle (θ) and azimuth angle (φ), and keeping the shear velocity non-zero to stabilize one-way wave extrapolation, the dispersion relation equation in 3D TTI media can be written as:

$$c_4 T_z^4 + c_3 T_z^3 + c_2 T_z^2 + c_1 T_z + c_0 = 0 \qquad (1)$$

where:

$$c_4 = f - 1 + 2\varepsilon \sin^2\theta (f-1) - \left(\frac{f}{2}(\varepsilon - \delta)\sin^2 2\theta\right)$$

$$c_3 = -\left((f-1)2\varepsilon \sin 2\theta - f(\varepsilon - \delta)\sin 4\theta\right)\left(T_x \cos\varphi - T_y \sin\varphi\right)$$

$$c_2 = \left(2(f-1)(1+\varepsilon) - f(\varepsilon-\delta)\left(2\cos^2 2a - \sin^2 2a\right)\right)\left(T_x \cos\varphi - T_y \sin\varphi\right)^2$$
$$+2\left((f-1)(1+\varepsilon) + (f-1)\varepsilon \sin^2\theta - f(\varepsilon-\delta)\cos^2\theta\right)\left(T_x \sin\varphi + T_y \cos\varphi\right)^2$$
$$+\left(2\varepsilon \sin^2\theta + 2 - f\right)$$

$$c_1 = \left(2\varepsilon \sin 2\theta (f-1) + f(\varepsilon-\delta)\sin 4\theta\right)\left(T_x \cos\varphi - T_y \sin\varphi\right)^3 +$$
$$+2\sin 2\theta\left((f-1)\varepsilon + f(\varepsilon-\delta)\right)\left(T_x \cos\varphi - T_y \sin\varphi\right)\left(T_x \sin\varphi + T_y \cos\varphi\right)^2$$
$$+2\varepsilon \sin 2\theta\left(T_x \cos\varphi - T_y \sin\varphi\right)$$

$$c_0 = \left((f-1)\left(1+2\varepsilon\cos^2\theta\right) - \frac{f}{2}(\varepsilon-\delta)\sin^2 2\theta\right)\left(T_x \cos\varphi - T_y \sin\varphi\right)^4$$
$$+(f-1)(1+2\varepsilon)\left(T_x \sin\varphi + T_y \cos\varphi\right)^4$$
$$+2\left((f-1)\left(1+\varepsilon+\varepsilon\cos^2\theta\right) - f(\varepsilon-\delta)\sin^2\theta\right)\left(T_x \cos\varphi - T_y \sin\varphi\right)^2\left(T_x \sin\varphi + T_y \cos\varphi\right)^2$$
$$+\left(2 - f + 2\varepsilon\cos^2\theta\right)\left(T_x \cos\varphi - T_y \sin\varphi\right)^2 + \left((2+2\varepsilon - f)\left(T_x \sin\varphi + T_y \cos\varphi\right)^2 - 1\right)$$

There exists four solutions, two of them are related to up and down-going P-waves and the other two are related to up and down-going S-waves. The TTI dispersion relation equation (1) includes the anisotropic parameters from step **101** for the prestack shot gather selected in step **102(b)**.

[0034] In step **106**, TTI coefficients are approximated using the TTI dispersion relation equation (1). One embodiment of a method **500** for approximating the TTI coefficients is described further in reference to **FIG. 5**.

In step **107**, a hybrid TTI-WEM and/or a well-known phase shift algorithm are applied in the F-X domain to the velocity model and anisotropic parameters for the prestack shot gather selected in step **102b**. If water is present in the velocity model and the migration depth is not below a subsurface where the water meets the earth, then only the phase shift algorithm is applied. If water is present in the velocity model and the migration depth is below a subsurface where the water meets the earth, then the hybrid TTI-WEM and the phase shift algorithm are applied. If water is not present in the velocity model, then only the hybrid TTI-WEM is applied. Because the velocity of water is a known constant, the anisotropic parameters are all zero when applying the phase shift algorithm. The hybrid TTI-WEM is applied from a surface of the earth or a subsurface where the water meets the earth to the migration depth. The phase shift algorithm is only applied from a water surface to a subsurface where the water meets the earth. In order to apply the hybrid TTI-WEM in the F-X domain, $T_x$, $T_y$ and $T_z$ from equation (8) are replaced by the partial differential operators $i\frac{\partial P}{\partial x}\frac{V}{\omega}$, $i\frac{\partial P}{\partial y}\frac{V}{\omega}$ and $i\frac{\partial P}{\partial z}\frac{V}{\omega}$, which produce the following equation:

$$\frac{\partial P}{\partial z} = i\frac{\omega}{V}\left( T_{z0} + \frac{a_1\left(\frac{V}{\omega}\frac{\partial P}{\partial x}\right)^2 + ic_1\frac{V}{\omega}\frac{\partial P}{\partial x}}{1 + b_1\frac{V}{\omega}\frac{\partial P}{\partial x}} + \frac{a_2\left(\frac{V}{\omega}\frac{\partial P}{\partial y}\right)^2 + ic_2\frac{V}{\omega}\frac{\partial P}{\partial y}}{1 + b_2\frac{V}{\omega}\frac{\partial P}{\partial y}} \right) \tag{2}$$

where P is the source side wavefield or the receiver side wavefield that must be propagated, V is velocity, ω is angular frequency, $T_{z0}$ is the solution for equation (1) when $T_x$ and $T_y$ are zero and $a_1$, $b_1$, $c_1$, $a_2$, $b_2$, $c_2$, are the values of the TTI coefficients from equation (8). Equation (2) can then be solved using a well-known implicit finite difference ("FD") algorithm and the following equations:

$$\frac{\partial P}{\partial z} = i\frac{\omega}{V}T_{z0} \tag{3.1}$$

$$\frac{\partial P}{\partial z} = i\frac{\omega}{V}\left(\frac{a_1\left(\frac{V}{\omega}\frac{\partial P}{\partial x}\right)^2 + ic_1\frac{V}{\omega}\frac{\partial P}{\partial x}}{1 + b_1\frac{V}{\omega}\frac{\partial P}{\partial x}}\right) \tag{3.2}$$

$$\frac{\partial P}{\partial z} = i\frac{\omega}{V}\left(\frac{a_2\left(\frac{V}{\omega}\frac{\partial P}{\partial y}\right)^2 + ic_2\frac{V}{\omega}\frac{\partial P}{\partial y}}{1 + b_2\frac{V}{\omega}\frac{\partial P}{\partial y}}\right) \tag{3.3}$$

Thus, the solution from equation (3.1), which is the value of P, is used as input to solve equation (3.2) and obtain the value of P, which is used as input to solve equation (3.3) and obtain the final value for P. In this manner, cascading is used with the implicit FD algorithm to obtain the final value of $P_1$ for source side wavefield propagation and the final value of $P_2$ for receiver side wavefield propagation. For source side wavefield propagation, the input is a Ricker wavelet (t). Assuming the source side wavefield is $P_1$ (iw, ix, iy, iz) and $P_1 = 0$, then $P_1$ (iw, ix, iy, iz) = $P_1$ (iw, ix, iy, iz) + Ricker wavelet (iw), which is used to solve for $P_1$ in equation (3.1). For receiver side wavefield propagation, the input is gather (t, x, y), which is the prestack shot gather selected in step **102b**. Assuming the receiver side wavefield is $P_2$ (iw, ix, iy, iz) and $P_2 = 0$, then $P_2$ (iw, ix, iy, iz) = $P_2$ (iw, ix, iy, iz) + gather (iw, ix, iy), which is used to solve for $P_2$ in equation (3.1). In order to apply the phase shift algorithm in the F-X domain when water is present in the velocity model, equation (3.1) is solved for $P_1$ and $P_2$. For source side wavefield propagation, the input is a Ricker wavelet (t). Assuming the source side wavefield is $P_1$ (iw, ix, iy, iz) and $P_1$

= 0, then $P_1$ (iw, ix, iy, iz) = $P_1$ (iw, ix, iy, iz) + Ricker wavelet (iw), which is used to solve for $P_1$ in equation (3.1). For receiver side wavefield propagation, the input is gather (t, x, y), which is the prestack shot gather selected in step **102b**. Assuming the receiver side wavefield is $P_2$ (iw, ix, iy, iz) and $P_2$ = 0, then $P_2$ (iw, ix, iy, iz) = $P_2$ (iw, ix, iy, iz) + gather (iw, ix, iy), which is used to solve for $P_2$ in equation (3.1). In this manner, $P_1$ and $P_2$ may be used as the input in equation (3.1) to solve for $P_1$ and $P_2$ when applying TTI-WEM in the FX-domain instead of using the assumed $P_1$ and $P_2$ described hereinabove when only hybrid TTI-WEM is applied.

[0035] In step **109**, the source side wavefield propagation value ($P_1$) and the receiver side wavefield propagation value ($P_2$) from the hybrid TTI-WEM and/or the phase shift algorithm in step **107** are converted from the F-X domain to the T-X domain using techniques well-known in the art such as, for example, an inverse fast fourier transform ("IFFT") algorithm.

[0036] In step **110**, the following zero-lag cross-correlation image condition equation is applied to form a partial output image ($I_{time}$ (x, y, z)) using $P_1$ and $P_2$ from the hybrid TTI-WEM and/or the phase shift algorithm in step **107**:

$$I_{time}(x, y, z) = \sum_{it=1}^{nt} P_1(x, y, z, it) * P_2(x, y, z, it) \qquad (4)$$

[0037] In step **111**, a hybrid TTI-RTM is applied in the T-X domain to the velocity model and anisotropic parameters for the prestack shot gather selected in step **102b**. The hybrid TTI-RTM is applied from the migration depth, which may be a surface of the earth if it is zero, to the extent of the velocity model. P1 and P2 from the hybrid TTI-WEM and/or the phase shift algorithm in step **107** are used as input to solve equation (5):

$$\frac{\partial^2 \sigma_H}{\partial t^2} = V_p^2(1+2\varepsilon)M'\sigma_H + (V_p^2 - V_{sv}^2)\sqrt{1+2\delta}N'\sigma_V + V_{sv}^2 N'\sigma_H$$
$$\frac{\partial^2 \sigma_V}{\partial t^2} = (V_p^2\sqrt{1+2\delta} - \frac{V_{sv}^2}{\sqrt{1+2\delta}})M'\sigma_H + V_p^2 N'\sigma_V + V_{sv}^2 M'\sigma_V \quad (5)$$

where:

$$M' = \left\{ \begin{array}{l} (1-\sin^2\theta\cos^2\varphi)\frac{\partial^2}{\partial x^2} + (1-\sin^2\theta\sin^2\varphi)\frac{\partial^2}{\partial y^2} + \sin^2\theta\frac{\partial^2}{\partial z^2} \\ -\sin 2\theta\sin\varphi\frac{\partial^2}{\partial y\partial z} - \sin 2\theta\cos\varphi\frac{\partial^2}{\partial x\partial z} - \sin^2\theta\sin 2\varphi\frac{\partial^2}{\partial x\partial y} \end{array} \right\}$$

$$N' = \left\{ \begin{array}{l} \sin^2\theta\cos^2\varphi\frac{\partial^2}{\partial x^2} + \sin^2\theta\sin^2\varphi\frac{\partial^2}{\partial y^2} + \cos^2\theta\frac{\partial^2}{\partial z^2} \\ +\sin 2\theta\sin\varphi\frac{\partial^2}{\partial y\partial z} + \sin 2\theta\cos\varphi\frac{\partial^2}{\partial x\partial z} + \sin^2\theta\sin 2\varphi\frac{\partial^2}{\partial x\partial y} \end{array} \right\}$$

and where $\sigma_H$, $\sigma_V$ are horizontal and vertical stress components, respectively, and $\theta$ and $\varphi$ are dip and azimuth angle, respectively. Equation (5) thus, may be solved using a well-known explicit FD algorithm in the manner described in International Patent Application Publication No. WO/2011/053327. When $\theta$ and $\varphi$ are set to zero with $\varepsilon$ and $\delta$, equations (1) and (8) become hybrid VTI-RTM schemes, when $\theta$, $\varphi$, $\varepsilon$, and $\delta$ are all set to zero, they will become traditional hybrid isotropic RTM schemes.

[0038] In step **112**, the zero-lag cross-correlation image condition equation (4) is applied to form a partial output image ($I_{time}$ (x, y, z)) using $P_1$ and $P_2$ from the hybrid TTI-RTM in step **111**.

[0039] In step **113**, low wave number and migration artifacts are removed from the partial output images in steps **110** and **112** by filtering and smoothing to generate amplitude consistent partial output images. A well-known low-wave number filter is applied to the partial output images from steps **110** and **112**, then each filtered partial output image is divided by the

source-side wavefield propagation value $P_1$ from step **111** to generate the amplitude consistent partial output images.

[0040] In step **114**, the method **100** determines if there are more prestack shot gathers from the seismic survey data in step **101**. If there are more prestack shot gathers, then the method **100** returns to step **102b** to select another prestack shot gather. If there are no more prestack shot gathers, then the method **100** proceeds to step **115**.

[0041] In step **115**, the amplitude consistent partial output images from each iteration of step **113** are stacked and displayed using techniques well-known in the art. As a result, noise will be significantly cancelled and the final image will be enhanced.

[0042] Referring now to **FIG. 5**, one embodiment of a method **500** is illustrated for performing step **106** in **FIG. 1**.

[0043] In step **502**, a Jenkins-Traub algorithm is applied to equation (1) to solve for $T_z$ which represents polynomial zeros that relate to a down-going P-wave.

[0044] In step **504**, the TTI dispersion relation equation (1) is split by Pade approximation into x and y directions. Equation (1) then becomes::

$$T_z \approx T_{z0} - \frac{\sum_{j=1}^{2n} \alpha_j T_x^j}{1-\sum_{i=1}^{n} \beta_i \left(T_x^2\right)^i} - \frac{\sum_{j=1}^{2n} \alpha_j T_y^j}{1-\sum_{i=1}^{n} \beta_i \left(T_y^2\right)^i} \tag{6}$$

In step **506**, a least square optimization method is applied to equation (6), which forms equation (7) and is solved for $\alpha_j$ and $\beta_i$ to ultimately approximate the TTI coefficients.

$$\min \int_{T_{y\min}}^{T_{y\max}} \int_{T_{x\min}}^{T_{x\max}} T_z - (T_{z0} - \frac{\sum_{j=1}^{2n} \alpha_j T_x^j}{1-\sum_{i=1}^{n} \beta_i \left(T_x^2\right)^i} - \frac{\sum_{j=1}^{2n} \alpha_j T_y^j}{1-\sum_{i=1}^{n} \beta_i \left(T_y^2\right)^i}) dT_x dT_y \tag{7}$$

A least square optimization method such as, for example, the well-known Bonded Variable Least Square optimization method may be used. Once $\alpha_j$ and $\beta_i$ are known, a second order Pade approximation may be used to approximate the TTI coefficients. For second order approximation, the maximum propagation angle is up to 50°. Thus, the upper limit of $T_x$ and $T_y$ for least square optimization is less than +0.85 and the lower limit of $T_x$ and $T_y$ is greater than -0.85. For fourth order approximation, the maximum propagation angle is up to 70°. Thus, the upper limit of $T_x$ and $T_y$ for least square optimization is less than +0.90 and the lower limit of $T_x$ and $T_y$ is greater than -0.90. Because the hybrid TTI-WEM may be applied in shallow places, second order approximation is satisfactory for good image quality, however, any order for approximation could be used. In this manner, a large propagation angle is obtainable over other well-known methods that produces better image quality. By second order Pade approximation, $\alpha_j$ and $\beta_i$ are transferred to approximate the TTI coefficients ($a_i$, $b_i$, $c_i$) in the following equation:

$$T_z = T_{z0} - \frac{a_1 T_x^2 + c_1 T_x}{1 - b_1 T_x^2} - \frac{a_2 T_y^2 + c_2 T_y}{1 - b_2 T_y^2} \quad (8)$$

The TTI coefficients ($a_i$, $b_i$, $c_i$) from equation (8) may be saved in respective tables before applying the hybrid TTI-WEM.

## EXAMPLES

[0045] In this example, hybrid TTI-RTM and conventional two-way TTI-RTM are applied to offshore data for a comparison of their resulting images. A phase shift algorithm was applied according to step **107** in **FIG. 1** from a water surface to a subsurface where the water meets the earth. The hybrid TTI-WEM was applied according to step **107** in **FIG. 1** from the subsurface to a migration depth of 2 km. The hybrid TTI-WEM was applied from 2 km to the extent of the velocity model at 16 km according to step **111** in **FIG. 1**. An image of the velocity

model is illustrated in **FIG. 2A**. The anisotropic parameters for the velocity model in **FIG. 2A** are illustrated in **FIGS. 2B**(ε), **2C**(δ) and **2D**(θ).

[0046] As illustrated by a comparison of **FIGS. 3A** and **3B** with **FIG. 3C**, the application of the hybrid TTI-RTM as a result of the method **100** in **FIG. 1** produces a much cleaner and clearer image (**FIG. 3C**) than the images produced by conventional techniques in isotropic media (**FIG. 3A**) and conventional techniques in VTI media (**FIG. 3B**). Moreover, the image in **FIG. 3C** is much cleaner and clearer than the image in **FIG. 3D** at the water layer, which was produced by a conventional two-way RTM in TTI media. For example, the image ghost within circle **302d** and circle **304d** in **FIG. 3D** is not as evident within circle **302c** and circle **304c** in **FIG. 3C**. In the example illustrated by **FIG. 3C**, hybrid TTI-RTM saves 20% computational time than conventional two-way TTI-RTM when the migration depth is set at 2 km out of a total 16 km. If the migration depth is set deeper, more computational time may be saved. In table 2 below, the relative computation time for hybrid TTI-RTM and two-way conventional TTI-RTM in isotropic, VTI and TTI media is illustrated for this example.

| | Two-Way TTI-RTM (s) | Hybrid TTI-RTM (s) |
|---|---|---|
| Isotropic | 1.0 | 0.75 |
| VTI | 2.0 | 1.63 |
| TTI | 4.0 | 2.75 |

Table 2

[0047] In another example, the application of the hybrid TTI-RTM is tested on 2007 TTI data from BP. The image in **FIG. 4A** illustrates the results of conventional two-way TTI-RTM. The image in **FIG. 4B** illustrates the hybrid TTI-RTM as a result of the method **100** in **FIG. 1**. Although the conventional two-way TTI-RTM image in **FIG. 4A** accurately illustrates a salt boundary, noise appears on the top of the image and an image ghost appears within the circle

**402a**. By applying hybrid TTI-RTM, the noise at the top of the image in **FIG. 4B** weakens and the image ghost within the circle **402b** beside a salt boundary is significantly reduced.

[0048] Hybrid TTI-RTM thus, will handle rugged topography and complex near surface layers by wave equation datuming. Conventional two-way TTI-RTM, however, cannot handle topography or must apply vertical static shift to the pre-stack shot gather. Wave equation datuming is therefore, more accurate than applying a vertical static shift, especially for areas where the velocity contrast between the near surface and the substratum is not large. Hybrid TTI-WEM will also generate better results than applying a vertical static shift.

## System Description

[0049] The present invention may be implemented through a computer-executable program of instructions, such as program modules, generally referred to as software applications or application programs executed by a computer. The software may include, for example, routines, programs, objects, components, and data structures that perform particular tasks or implement particular abstract data types. The software forms an interface to allow a computer to react according to a source of input. SeisSpace™, which is a commercial software application marketed by Landmark Graphics Corporation, may be used as an interface application to implement the present invention. The software may also cooperate with other code segments to initiate a variety of tasks in response to data received in conjunction with the source of the received data. The software may be stored and/or carried on any variety of memory media such as CD-ROM, magnetic disk, bubble memory and semiconductor memory (*e.g.*, various types of RAM or ROM). Furthermore, the software and its results may be transmitted over a variety of carrier media such as optical fiber, metallic wire, free space and/or through any of a variety of networks such as the Internet.

[0050] Moreover, those skilled in the art will appreciate that the invention may be practiced with a variety of computer-system configurations, including hand-held devices, multiprocessor systems, microprocessor-based or programmable-consumer electronics, minicomputers, mainframe computers, and the like. Any number of computer-systems and computer networks are acceptable for use with the present invention. The invention may be practiced in distributed-computing environments where tasks are performed by remote-processing devices that are linked through a communications network. In a distributed-computing environment, program modules may be located in both local and remote computer-

storage media including memory storage devices. The present invention may therefore, be implemented in connection with various hardware, software or a combination thereof, in a computer system or other processing system.

[0051] Referring now to **FIG. 6**, a block diagram of a system for implementing the present invention on a computer is illustrated. The system includes a computing unit, sometimes referred to as a computing system, which contains memory, application programs, a client interface, a video interface and a processing unit that includes a graphics processor or graphics card. The computing unit is only one example of a suitable computing environment and is not intended to suggest any limitation as to the scope of use or functionality of the invention.

[0052] The memory primarily stores the application programs, which may also be described as program modules containing computer-executable instructions, executed by the computing unit for implementing the present invention described herein and illustrated in **FIGS. 1-5**. The memory therefore, includes a hybrid TTI-WEM module and a hybrid TTI-RTM module, which enable the method illustrated and described in reference to **FIG. 1**. and integrates functionality from the remaining application programs illustrated in **FIG. 6**. The hybrid TTI-WTM module therefore, may be used to implement steps **104-110** in **FIG. 1** and the hybrid TTI-RTM module may be used to implement steps **111-113** in **FIG. 1**. Alternatively, the TTI-WEM module and the TTI-RTM module may be combined into a single module to implement steps **104-113** in **FIG. 1**. The memory also includes SeisSpace,™ which may be used as an interface application to supply input data to the hybrid TTI-WEM module and the hybrid TTI-RTM module and/or display the data results from the hybrid TTI-WEM module and the hybrid TTI-RTM module. SeisSpace™, therefore, may be used to implement steps **101-102b** and **114-115** in **FIG. 1**. Although SeisSpace™ may be used as an interface application, other interface

applications may be used, instead, or each hybrid TTI-WEM module and hybrid TTI-RTM module may be used as a stand-alone application.

[0053] Although the computing unit is shown as having a generalized memory, the computing unit typically includes a variety of computer readable media. By way of example, and not limitation, computer readable media may comprise computer storage media and communication media. The computing system memory may include computer storage media in the form of volatile and/or nonvolatile memory such as a read only memory (ROM) and random access memory (RAM). A basic input/output system (BIOS), containing the basic routines that help to transfer information between elements within the computing unit, such as during start-up, is typically stored in ROM. The RAM typically contains data and/or program modules that are immediately accessible to, and/or presently being operated on, the processing unit. By way of example, and not limitation, the computing unit includes an operating system, application programs, other program modules, and program data.

[0054] The components shown in the memory may also be included in other removable/nonremovable, volatile/nonvolatile computer storage media or they may be implemented in the computing unit through an application program interface ("API") or cloud computing, which may reside on a separate computing unit connected through a computer system or network. For example only, a hard disk drive may read from or write to nonremovable, nonvolatile magnetic media, a magnetic disk drive may read from or write to a removable, nonvolatile magnetic disk, and an optical disk drive may read from or write to a removable, nonvolatile optical disk such as a CD ROM or other optical media. Other removable/non-removable, volatile/nonvolatile computer storage media that can be used in the exemplary operating environment may include, but are not limited to, magnetic tape cassettes,

flash memory cards, digital versatile disks, digital video tape, solid state RAM, solid state ROM, and the like. The drives and their associated computer storage media discussed above provide storage of computer readable instructions, data structures, program modules and other data for the computing unit.

[0055] A client may enter commands and information into the computing unit through the client interface, which may be input devices such as a keyboard and pointing device, commonly referred to as a mouse, trackball or touch pad. Input devices may include a microphone, joystick, satellite dish, scanner, or the like. These and other input devices are often connected to the processing unit through the client interface that is coupled to a system bus, but may be connected by other interface and bus structures, such as a parallel port or a universal serial bus (USB).

[0056] A monitor or other type of display device may be connected to the system bus via an interface, such as a video interface. A graphical user interface ("GUI") may also be used with the video interface to receive instructions from the client interface and transmit instructions to the processing unit. In addition to the monitor, computers may also include other peripheral output devices such as speakers and printer, which may be connected through an output peripheral interface.

[0057] Although many other internal components of the computing unit are not shown, those of ordinary skill in the art will appreciate that such components and their interconnection are well-known.

[0058] While the present invention has been described in connection with presently preferred embodiments, it will be understood by those skilled in the art that it is not intended to limit the invention to those embodiments. It is therefore, contemplated that various alternative

embodiments and modifications may be made to the disclosed embodiments without departing from the scope of the invention defined by the appended claims and equivalents thereof.

# CLAIMS

1. A method for imaging seismic data, which comprises:

approximating TTI coefficients using a Pade approximation and a dispersion relation equation;

applying hybrid TTI-WEM to a velocity model and anisotropic parameters for a pre-stack shot gather using the approximated TTI coefficients and a computer system to determine a source side wavefield propagation value and a receiver side wavefield propagation value in a frequency-space domain;

converting the source side wavefield propagation value and the receiver side wavefield propagation value from the frequency-space domain to a time-space domain; and

applying a zero-lag cross-correlation image condition equation to form a partial output image using the converted source side wavefield propagation value and the converted receiver side wavefield propagation value.

2. The method of claim 1, further comprising:

applying hybrid TTI-RTM to the velocity model and the anisotropic parameters for the pre-stack shot gather using the converted source side wavefield propagation value and the converted receiver side wavefield propagation value to determine another source side wavefield propagation value and another receiver side wavefield propagation value in the time-space domain; and

applying the zero-lag cross-correlation image condition equation to form another partial output image using the another source side wavefield propagation value and the another receiver side wavefield propagation value.

3. The method of claim 2, further comprising:

stacking each partial output image; and

displaying the stacked partial output images.

4. The method of claim 1, wherein the dispersion relation equation is created from a phase velocity function and a rotation matrix.

5. The method of claim 2, further comprising applying a phase shift algorithm to the velocity model and the anisotropic parameters for the pre-stack shot gather before applying the hybrid TTI-WEM to determine the source side wavefield propagation value and the receiver side wavefield propagation value.

6. The method of claim 5, further comprising setting a migration depth between the hybrid TTI-WEM and the hybrid TTI-RTM.

7. The method of claim 6, wherein the phase shift algorithm is applied to the velocity model and the anisotropic parameters from a water surface to a subsurface where the water meets earth.

8. The method of claim 6, wherein the hybrid TTI-WEM is applied to the velocity model and the anisotropic parameters from an earth surface or a subsurface where water meets the earth to the migration depth.

9. The method of claim 6, wherein the hybrid TTI-RTM is applied to the velocity model and the anisotropic parameters from the migration depth to an extent of the velocity model.

10. The method of claim 2, further comprising:

filtering and smoothing each partial output image to generate a respective amplitude-consistent partial output image;

stacking each amplitude-consistent partial output image; and

displaying the stacked amplitude-consistent partial output images.

11. A non-transitory computer-readable medium carrying computer executable instructions for imaging seismic data, the instructions being executable to implement:

approximating TTI coefficients using a Pade approximation and a dispersion relation equation;

applying hybrid TTI-WEM to a velocity model and anisotropic parameters for a pre-stack shot gather using the approximated TTI coefficients and a computer system to determine a source side wavefield propagation value and a receiver side wavefield propagation value in a frequency-space domain;

converting the source side wavefield propagation value and the receiver side wavefield propagation value from the frequency-space domain to a time-space domain; and

applying a zero-lag cross-correlation image condition equation to form a partial output image using the converted source side wavefield propagation value and the converted receiver side wavefield propagation value.

12. The computer-readable medium of claim 11, further comprising:

applying hybrid TTI-RTM to the velocity model and the anisotropic parameters for the pre-stack shot gather using the converted source side wavefield propagation value and the converted receiver side wavefield propagation value to determine another source side wavefield propagation value and another receiver side wavefield propagation value in the time-space domain; and

applying the zero-lag cross-correlation image condition equation to form another partial output image using the another source side wavefield propagation value and the another receiver side wavefield propagation value.

13. The computer-readable medium of claim 12, further comprising:

stacking each partial output image; and

displaying the stacked partial output images.

14. The computer-readable medium of claim 11, wherein the dispersion relation equation is created from a phase velocity function and a rotation matrix.

15. The computer-readable medium of claim 12, further comprising applying a phase shift algorithm to the velocity model and the anisotropic parameters for the pre-stack shot gather before applying the hybrid TTI-WEM to determine the source side wavefield propagation value and the receiver side wavefield propagation value.

16. The computer-readable medium of claim 15, further comprising setting a migration depth between the hybrid TTI-WEM and the hybrid TTI-RTM.

17. The computer-readable medium of claim 16, wherein the phase shift algorithm is applied to the velocity model and the anisotropic parameters from a water surface to a subsurface where the water meets earth.

18. The computer-readable medium of claim 16, wherein the hybrid TTI-WEM is applied to the velocity model and the anisotropic parameters from an earth surface or a subsurface where water meets the earth to the migration depth.

19. The computer-readable medium of claim 16, wherein the hybrid TTI-RTM is applied to the velocity model and the anisotropic parameters from the migration depth to an extent of the velocity model.

20. The computer-readable medium of claim 12, further comprising:

filtering and smoothing each partial output image to generate a respective amplitude-consistent partial output image;

stacking each amplitude-consistent partial output image; and

displaying the stacked amplitude-consistent partial output images.

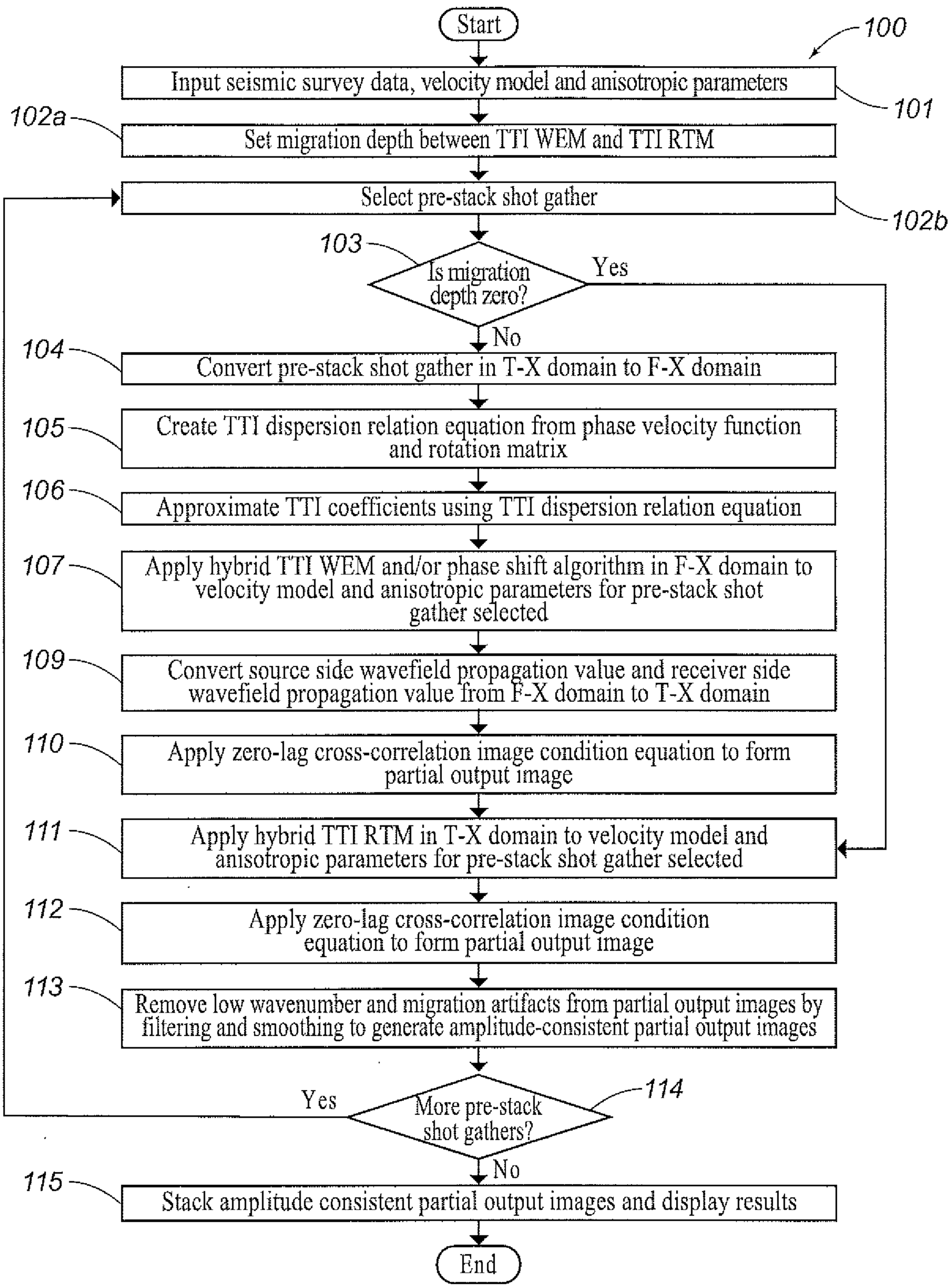
Start
100
Input seismic survey data, velocity model and anisotropic parameters
101
102a
Set migration depth between TTI WEM and TTI RTM
Select pre-stack shot gather
102b
103
Is migration depth zero?
Yes
No
104
Convert pre-stack shot gather in T-X domain to F-X domain
105
Create TTI dispersion relation equation from phase velocity function and rotation matrix
106
Approximate TTI coefficients using TTI dispersion relation equation
107
Apply hybrid TTI WEM and/or phase shift algorithm in F-X domain to velocity model and anisotropic parameters for pre-stack shot gather selected
109
Convert source side wavefield propagation value and receiver side wavefield propagation value from F-X domain to T-X domain
110
Apply zero-lag cross-correlation image condition equation to form partial output image
111
Apply hybrid TTI RTM in T-X domain to velocity model and anisotropic parameters for pre-stack shot gather selected
112
Apply zero-lag cross-correlation image condition equation to form partial output image
113
Remove low wavenumber and migration artifacts from partial output images by filtering and smoothing to generate amplitude-consistent partial output images
Yes
More pre-stack shot gathers?
114
No
115
Stack amplitude consistent partial output images and display results
End

FIG. 1

FIG. 2A

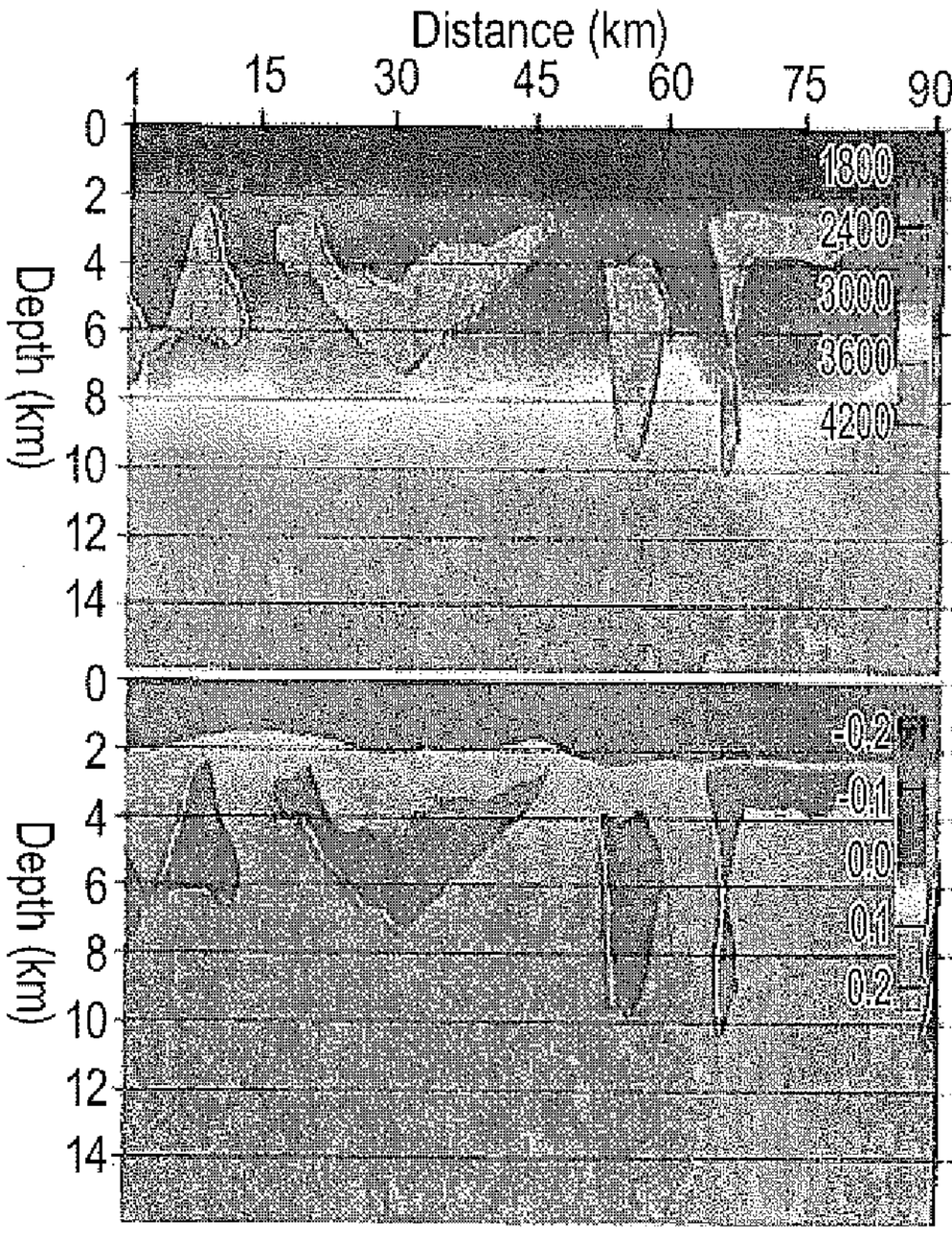


FIG. 2B

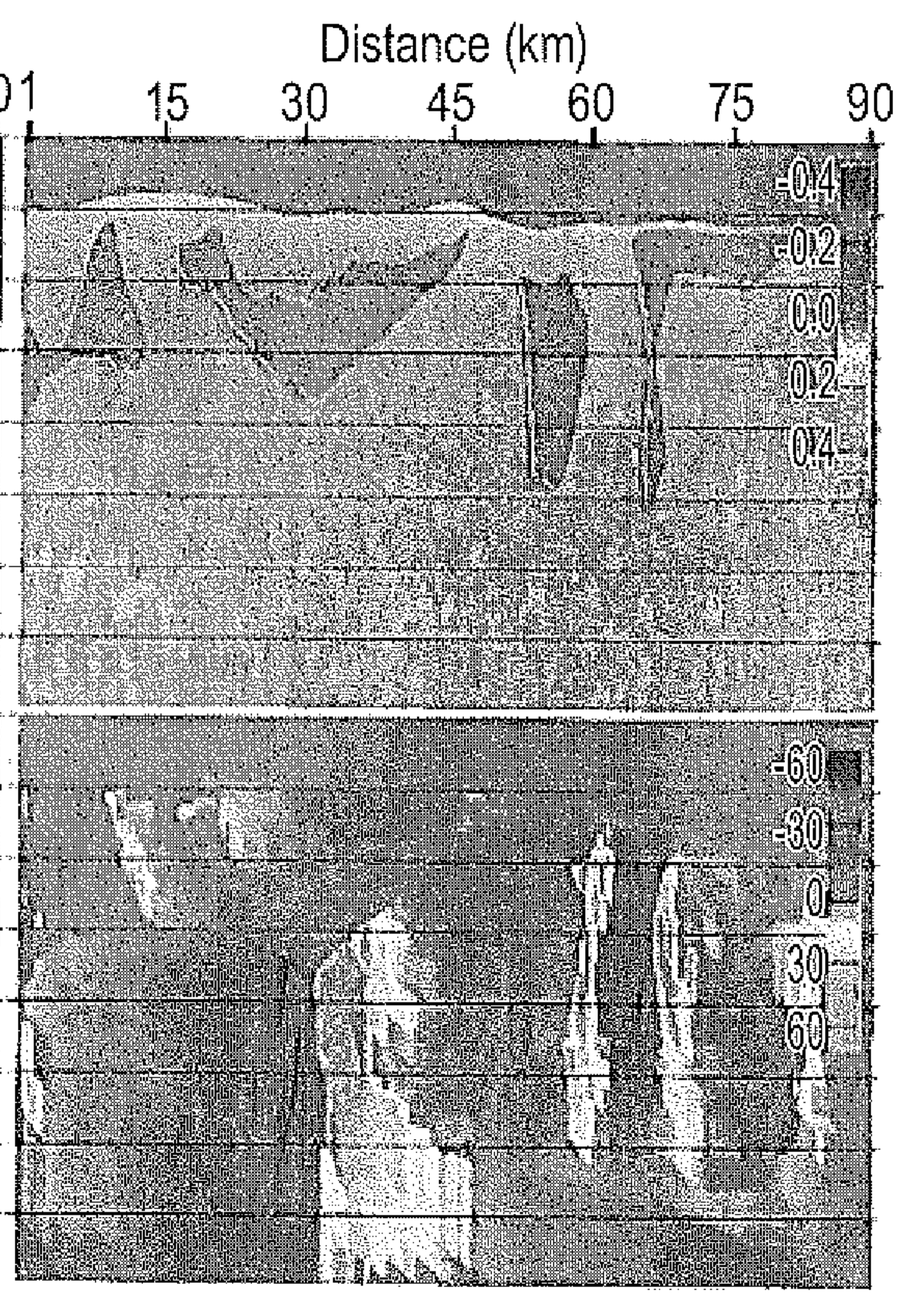


FIG. 2C




FIG. 2D

FIG. 3A

FIG. 3B

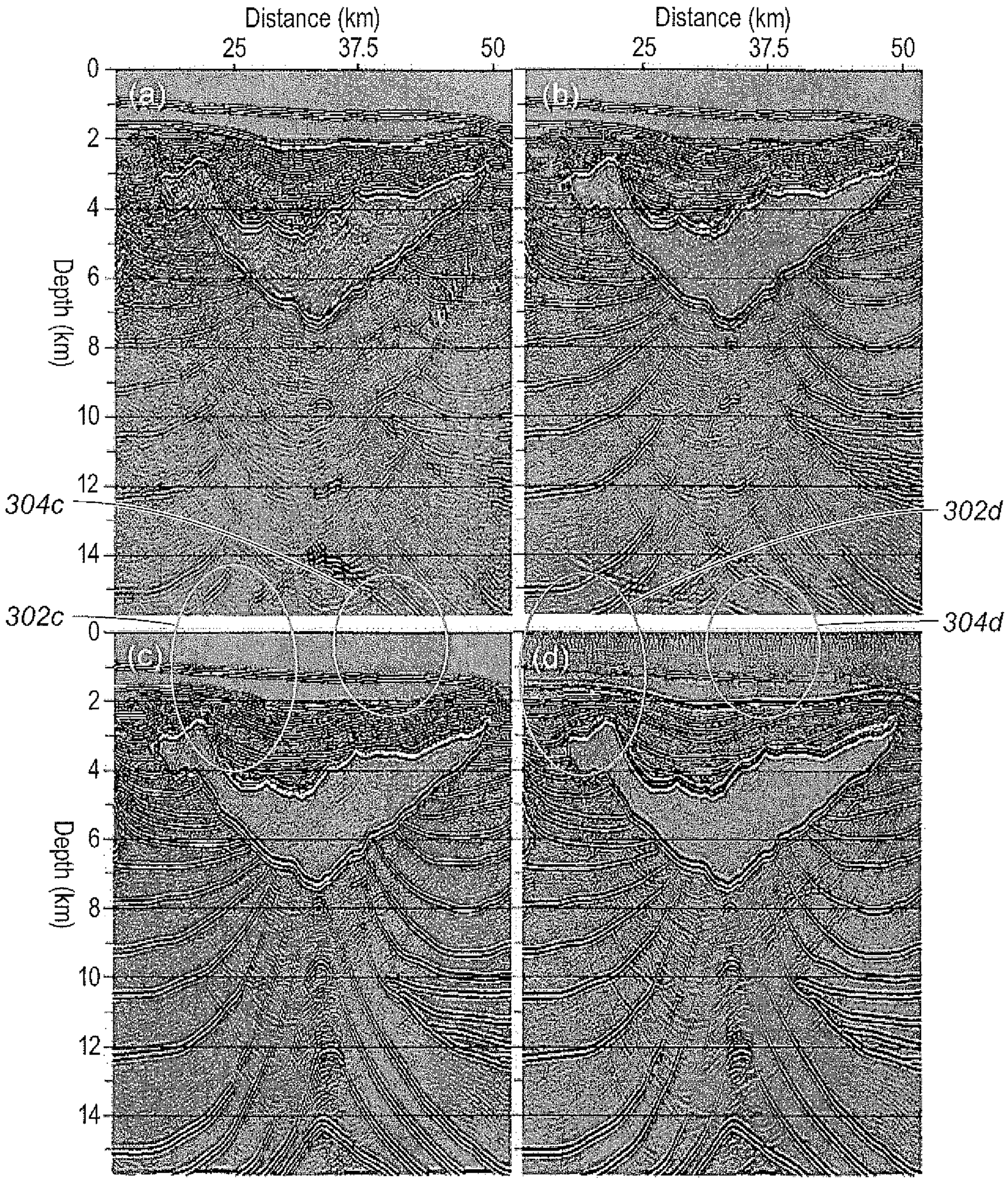


FIG. 3C

FIG. 3D

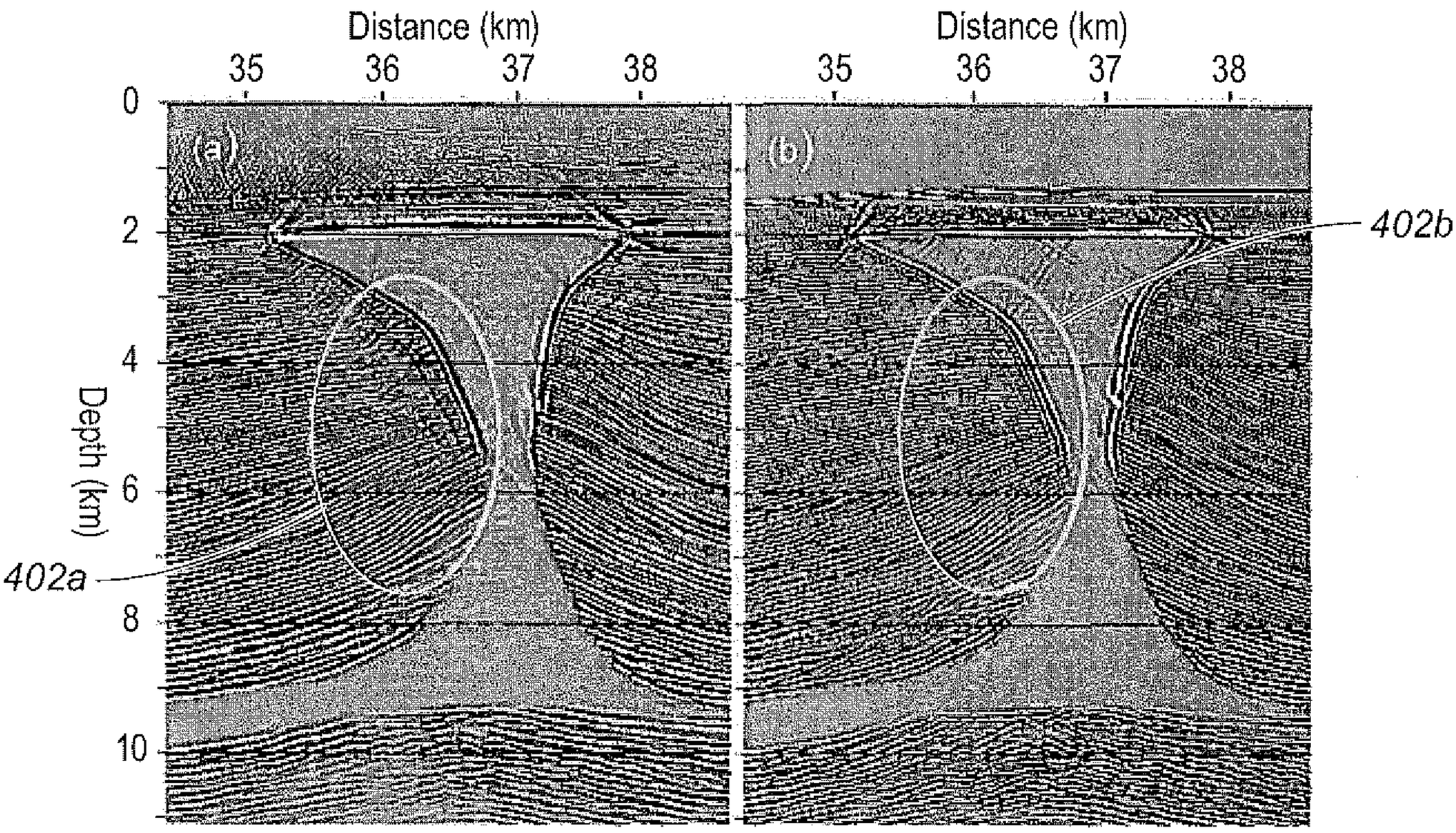


FIG. 4A FIG. 4B

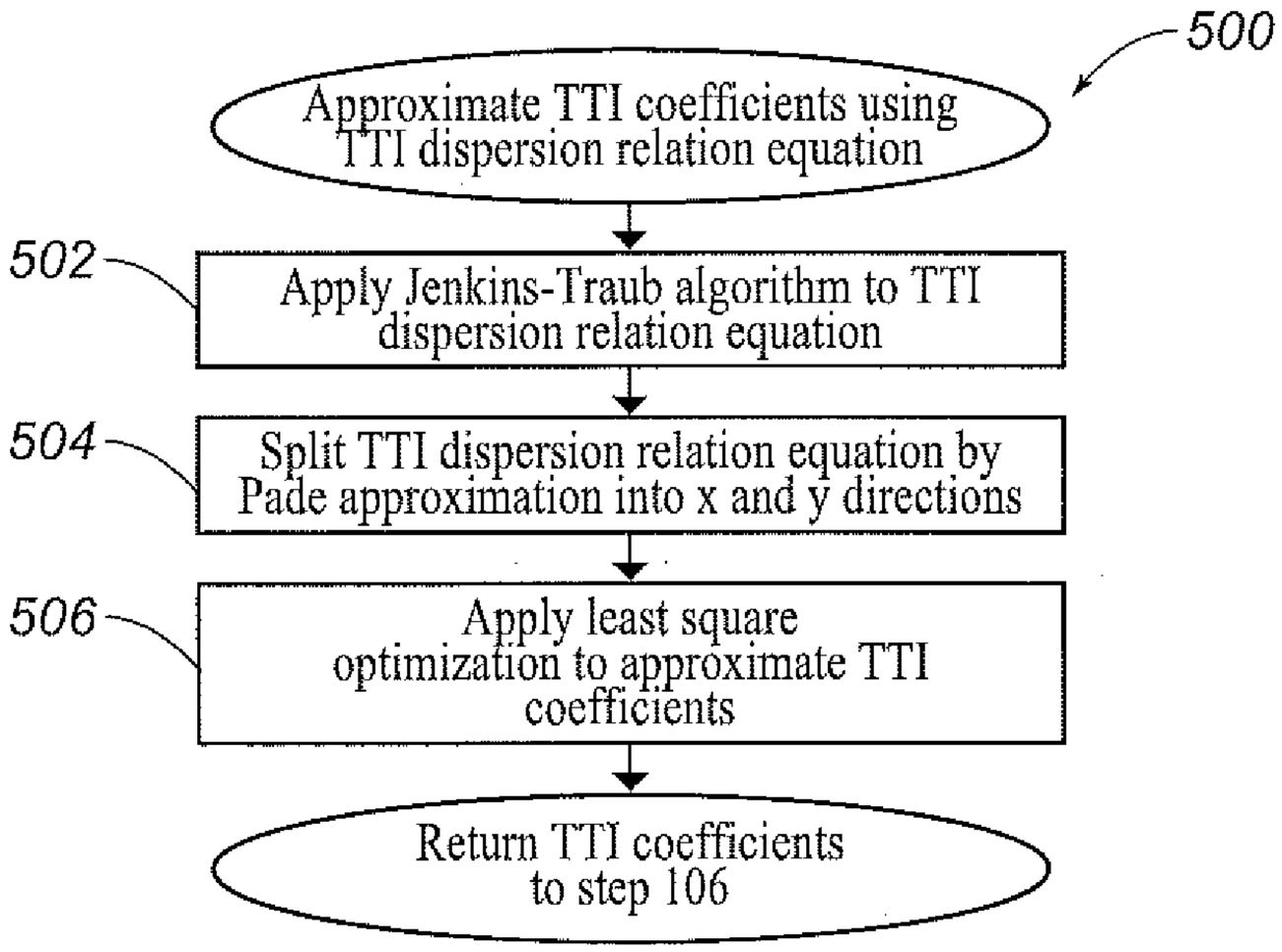


FIG. 5

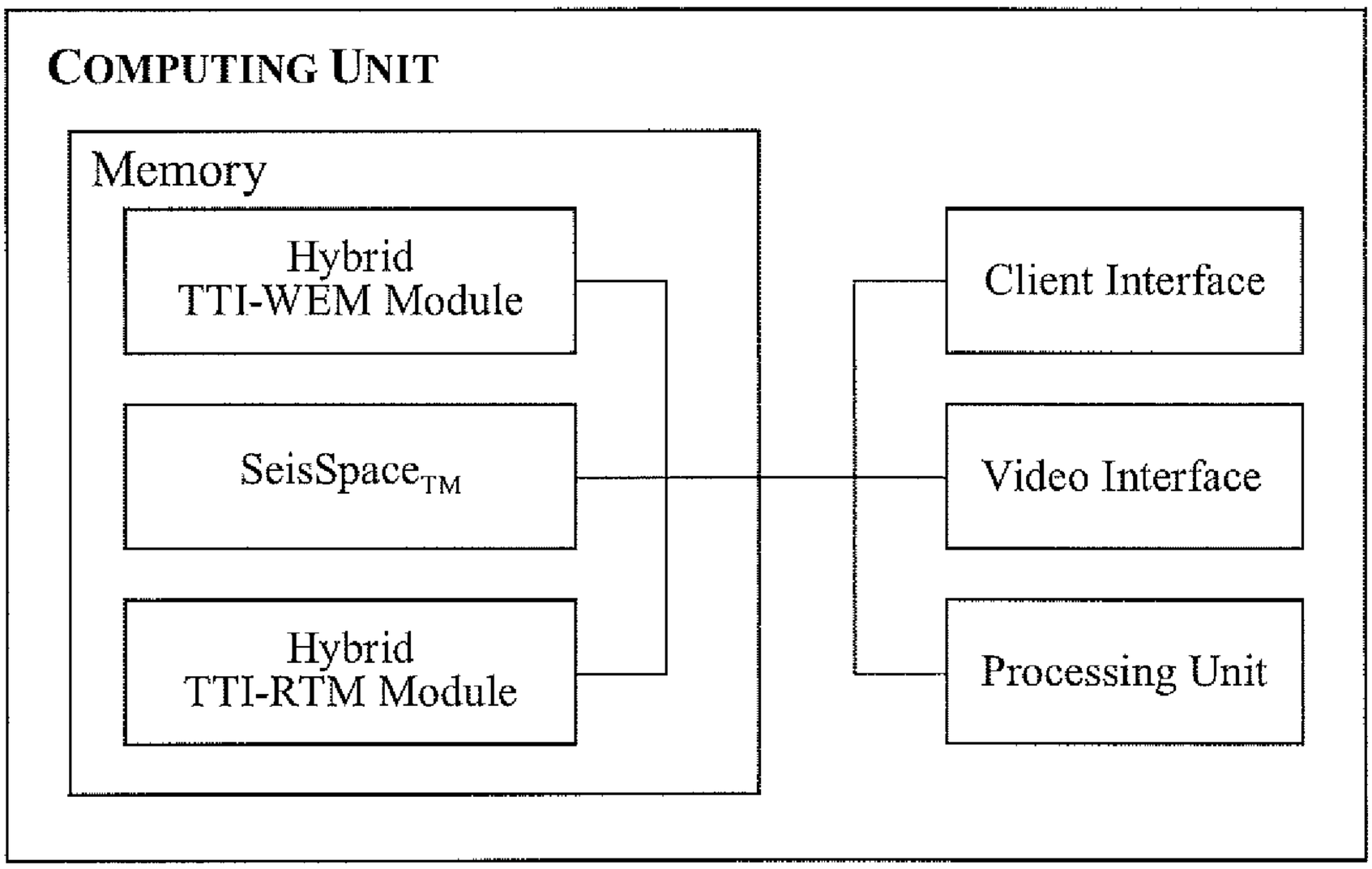
COMPUTING UNIT
Memory
Hybrid
TTI-WEM Module
SeisSpace™
Hybrid
TTI-RTM Module
Client Interface
Video Interface
Processing Unit

FIG. 6

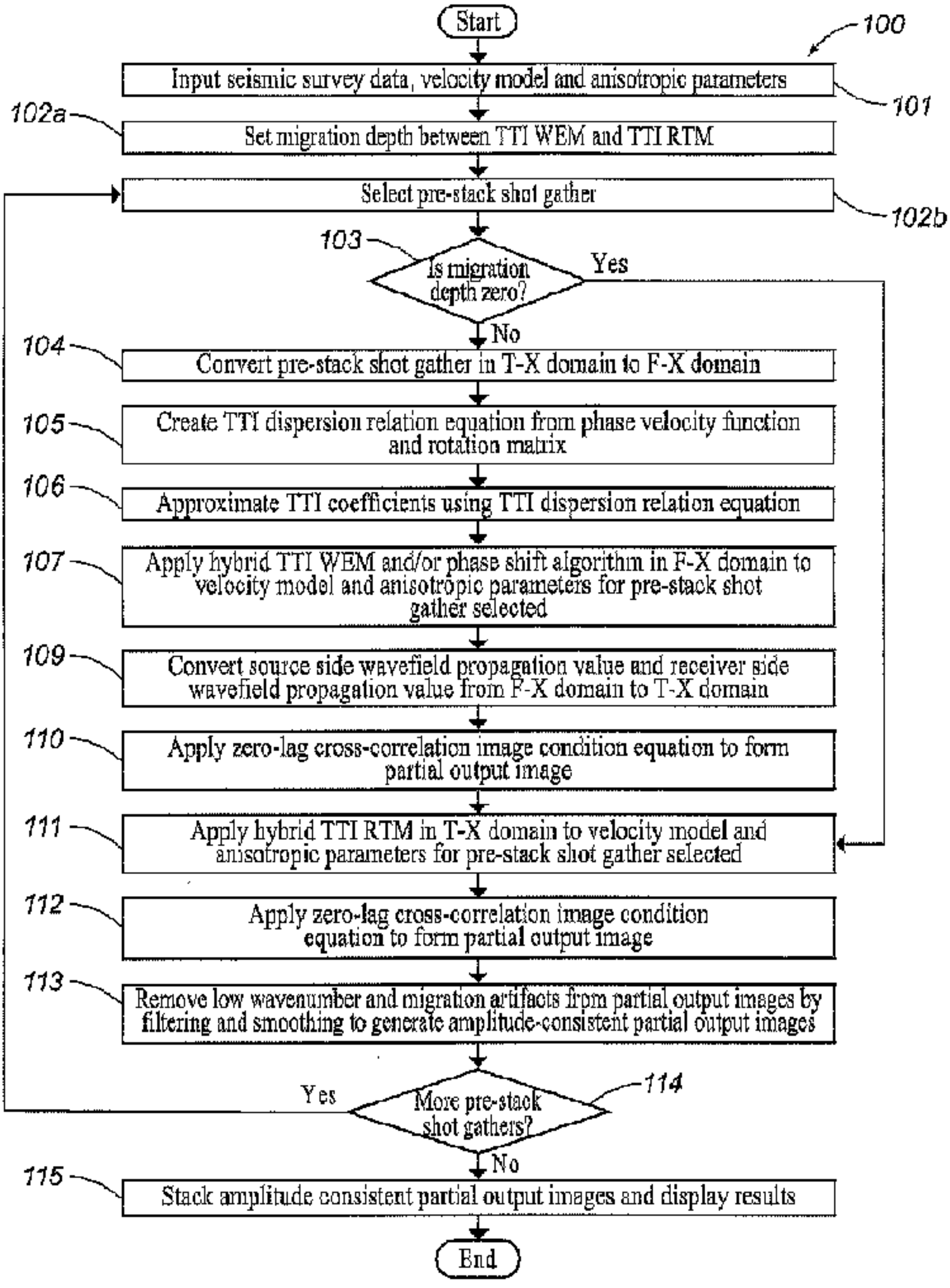
Start
100
Input seismic survey data, velocity model and anisotropic parameters
101
102a
Set migration depth between TTI WEM and TTI RTM
Select pre-stack shot gather
102b
103
Is migration depth zero?
Yes
No
104
Convert pre-stack shot gather in T-X domain to F-X domain
105
Create TTI dispersion relation equation from phase velocity function and rotation matrix
106
Approximate TTI coefficients using TTI dispersion relation equation
107
Apply hybrid TTI WEM and/or phase shift algorithm in F-X domain to velocity model and anisotropic parameters for pre-stack shot gather selected
109
Convert source side wavefield propagation value and receiver side wavefield propagation value from F-X domain to T-X domain
110
Apply zero-lag cross-correlation image condition equation to form partial output image
111
Apply hybrid TTI RTM in T-X domain to velocity model and anisotropic parameters for pre-stack shot gather selected
112
Apply zero-lag cross-correlation image condition equation to form partial output image
113
Remove low wavenumber and migration artifacts from partial output images by filtering and smoothing to generate amplitude-consistent partial output images
114
More pre-stack shot gathers?
Yes
No
115
Stack amplitude consistent partial output images and display results
End